Microfluidic Synthesis of Elastomeric Microparticles: A Case Study in Catalysis of Palladium-Mediated Cross-Coupling

Jeffrey A. Bennett, Andrew J. Kristof, Vishal Vasudevan, Jan Genzer, Jiri Srogl, and Milad Abolhasani
Dept. of Chemical and Biomolecular Engineering, North Carolina State University, Raleigh, NC 27695

DOI 10.1002/aic.16119
Published online in Wiley Online Library (wileyonlinelibrary.com)

Palladium (Pd)-loaded poly-hydromethylsiloxane (PHMS) microparticles of tunable size and elasticity are prepared in a capillary-based coaxial flow-focusing microfluidic device constructed using off-the-shelf components. Simultaneous droplet formation and chemical cross-linking processes are performed by tuning the dilution of the cross-linking catalyst in the annular flow of the microreactor, resulting in PHMS microparticles synthesized in a single step. The size of the elastomeric microparticles can be tuned by adjusting the flow rate ratio of the polymer and cross-linker mixture to water, while the elasticity can be tuned by the polymer to cross-linker ratio as well as the flow rate ratio of the polymer mixture to cross-linking catalyst mixture. Microparticle elasticity is characterized by the degree of solvent uptake. Application of the synthesized PHMS microparticles in organic synthesis is demonstrated by producing monodispersed Pd-loaded microparticles and utilizing them as microreaction vessels for continuous Suzuki-Miyaura cross-coupling in a Pd-loaded microparticle-packed bed reactor. *AIChE J*, 00: 000–000, 2018
Keywords: microfluidics, reactor analysis, cross-coupling, interfacial processes, multiphase flow, polymerization

Introduction

Metal-mediated cross-coupling reactions are valuable tools to organic chemists and play a critical role in synthesizing numerous complex chemical compounds in the pharmaceutical industry.[1] Flow chemistry has recently emerged as an effective strategy for continuous manufacturing of pharmaceutical targets.[2,3] However, the current limitations of continuous flow chemistry approaches necessitate the development of more efficient and environmentally friendly continuous flow technologies for organic synthesis. These challenges include extensive utilization of volatile and toxic organic solvents, catalyst recovery in the case of homogenous catalysis, and complex immobilization chemistry.

Recently, it has been demonstrated that Pd-loaded poly-hydromethylsiloxane (PHMS) elastomers can be utilized as the catalyst for heterogenous carbon-carbon cross-coupling reactions in batch.[4] The Pd nanoparticles were generated inside the bulk PHMS gel by diffusion of a Pd acetate solution dissolved in toluene. Once in the PHMS gel, the Pd^{2+} was reduced to catalytically active Pd^0 available for cross-coupling chemistry. Immobilized heterogeneous catalyst for cross-coupling removes the need of an energy-intensive separation step to recover the catalyst from the reaction mixture. The loaded Pd in PHMS gel also has the advantage of using solvents that are less harsh than those used in the conventional metal-mediated cross-coupling reactions (i.e., ethanol instead of toluene). In addition, the catalyst loaded permanently on a porous scaffold can be incorporated into well-known processes like a PBR. However, the large variation in size associated with conventional emulsion-based polymerization (bottom-to-top) and bulk gel mechanical breakup (top-to-bottom) approaches makes it challenging to use these promising organic synthesis scaffolds (i.e., silicone elastomers) in a continuous flow chemistry setup. Polydispersed packing of silicone elastomer particles (from batch emulsion or mechanical breakup) results in a large pressure drop across the bed which can in turn deform the elastomer particles, causing blockages and even higher operation pressures.[5]

Over the past decade, multiphase microfluidic strategies, owing to their consistent microdroplet formation and high-throughput production capabilities, have been utilized for synthesis of a wide range of microparticles including hydrogels[6–11] and microgels.[12–15] Polymerization of microgels is typically conducted in two discrete steps, a droplet generation, followed by a cross-linking initiation through a temperature gradient,[16] UV light irradiation,[7,17] or chemical reaction in the presence of a polymerization catalyst.[18] The separation of the temperature stimulation or UV light irradiation zone from the microdroplet formation step, make them ideal for on-chip polymerization of compatible polymers [e.g., poly(acrylamide), through photoinitiation, and poly(*N*-isopropylacrylamide), through thermal initiation]. However, the PHMS required for the reduction of the Pd, has several properties that make it difficult to synthesize microparticles using conventional microfluidic methods. PHMS is only cross-linked by hydrosilylation, a chemical method with no thermal or photoinitiators, with rapid reaction kinetics and unfavorable solubility in aqueous solution. Microparticles must be made and cross-linked in a single process step as the catalyst solubility requires mixing in the dispersed phase before droplet

Additional Supporting Information may be found in the online version of this article.

Correspondence concerning this article should be addressed to M. Abolhasani at abolhasani@ncsu.edu.

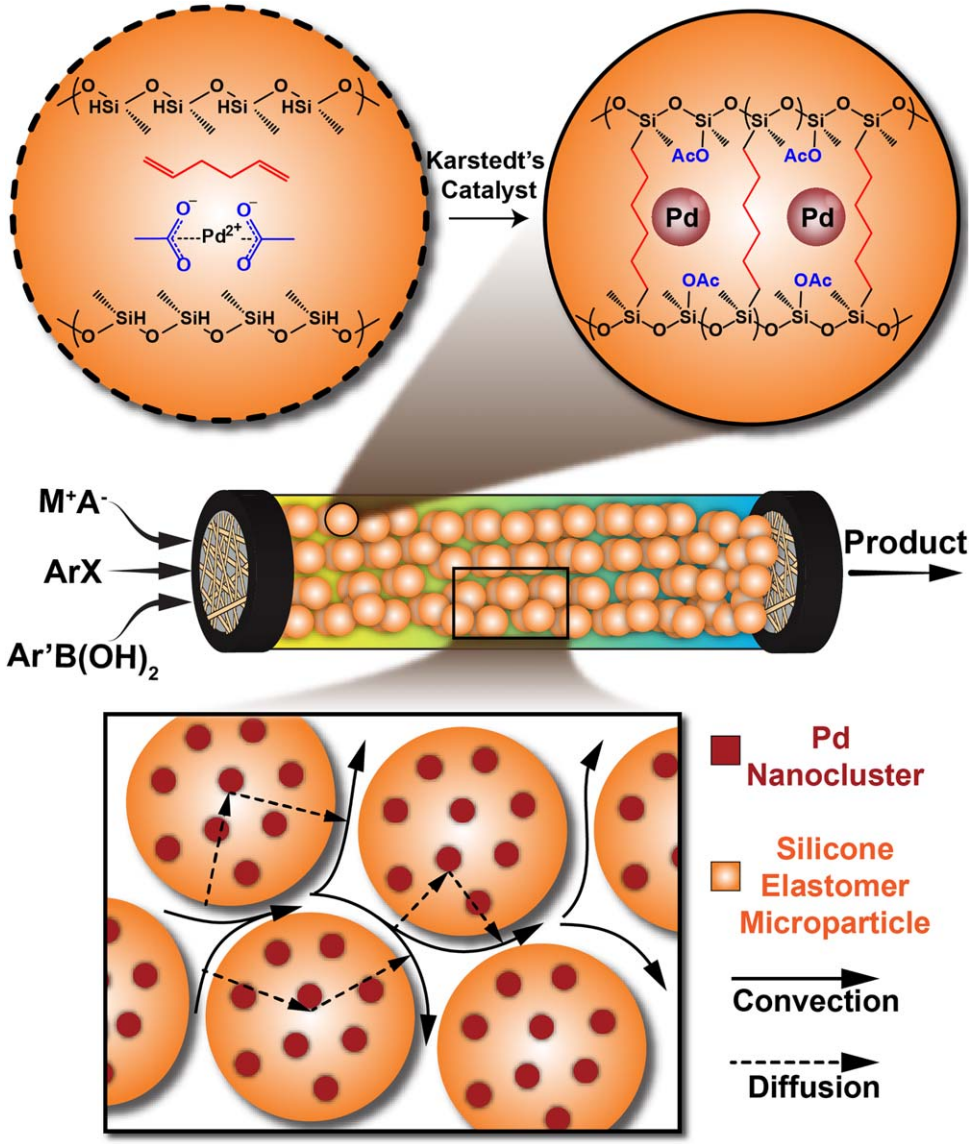

Figure 1. Schematic of Pd-loaded PHMS microparticle synthesis by hydrosilylation cross-coupling and construction of the μ-PBR.

[Color figure can be viewed at wileyonlinelibrary.com]

breakup, and the fast reaction poses risk for on-chip microdroplet formation as the polymerization might cause clogging of microchannels within seconds of operation. Additionally, PHMS is incompatible with conventional polydimethylsiloxane (PDMS)-based microfluidic devices without extreme surface functionalization. We hope to address some of the difficulties of on-chip cross-linking for the production of chemically cross-linked elastomeric microparticles as well as to expand the range of available polymers to include siloxanes which can be difficult to produce in conventional PDMS or thermoplastic-based devices.

In this work, we design and develop a multiphase microfluidic strategy to address the afore-mentioned challenges of the on-chip chemical cross-linking approach for high-throughput production of silicone elastomer microparticles with tunable size, elasticity, and loading capacity. Utilizing the developed microfluidic platform, we synthesize monodispersed microscale scaffolds (i.e., PHMS microparticles) for continuous flow heterogenous catalysis. Elastomeric microparticles loaded with a metal catalyst (Pd) are then loaded in a tubular Teflon reactor to construct a microparticle-packed bed reactor (μ-PBR) (Figure 1). The μ-PBR offers an increase in catalytic surface area and improved mass transport within the continuous flow reactor for biphasic C-C cross-coupling reactions while maintaining the Pd-loaded elastomer's catalytic activity and the benefits of flow processes over batch methods.[19–21]

Experimental

Chemicals

Toluene (anhydrous, 99.8%), sodium dodecyl sulfate (SDS), palladium (II) diacetate ($\geq$99.9% trace metals), silver acetate, PHMS (average Mn 1700–3200), 1,5-hexadiene, and platinum(0)-1,3-divinyl-1,1,3,3-tetramethly-disiloxane (Karstedt's catalyst) (in xylene, Pt-2%) were purchased from Sigma Aldrich. Acetone and 2-propanol (IPA) were purchased from VWR Analytical. The following cross-coupling reagents were received from Sigma Aldrich: potassium carbonate

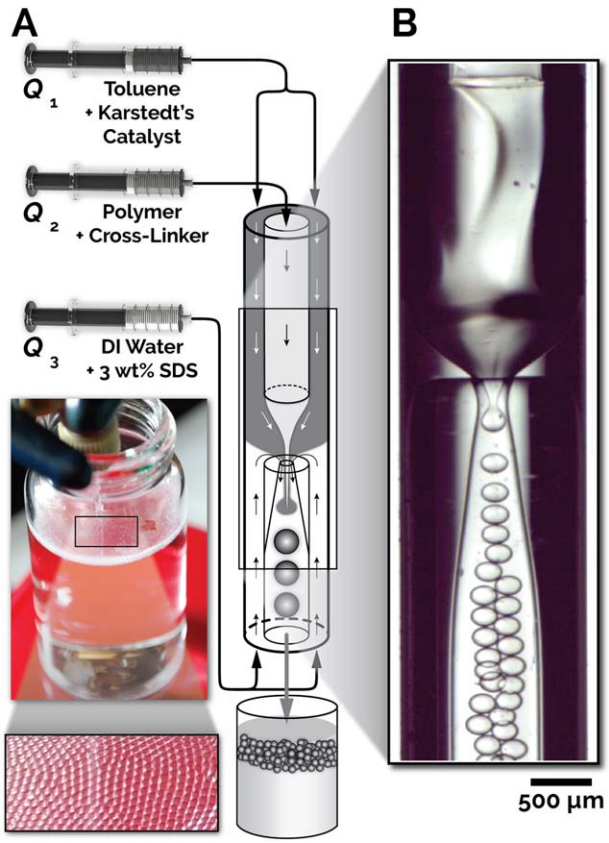

Figure 2. (A) Schematic of the experimental setup utilized for the continuous production of the PHMS microparticles. The inset shows the collection vial at the bottom of the microreactor. (B) A bright-field optical micrograph of the 3-D flow-focusing microreactor during microparticle synthesis.

10 μL/min Q_1, 10 μL/min Q_2, and 60 μL/min Q_3. [Color figure can be viewed at wileyonlinelibrary.com]

(K_2CO_3), ethanol (EtOH), phenylboronic acid, 4-iodotoluene, naphthalene, and 4-phenyltoluene. All chemicals were used as received. Deionized (DI) water was obtained in-house using a PURELAB Flex purification system (Elga).

Elastomeric microparticle production microreactor construction

A 3-D flow-focusing microreactor, shown in Figure 2, was constructed using commercially available components with only minor modifications. The device consists of three glass capillaries (Friedrich & Dimmock): (i) a round, outer capillary (1.5 mm outer diameter [OD], 1.12 mm inner diameter [ID], and 100 mm in length), which was cut to 50 mm in length; (ii) a round, inner capillary (1 mm OD, 0.5 mm ID, and 100 mm long), cut to 40 mm long; and (iii) a flamed-tip inner capillary, initial dimensions (1 mm OD, 0.5 mm ID, and 100 mm long), produced using a dual-stage glass micropipette puller (Narishige, PC-10). A cross-section of the flow-focusing microreactor is shown in Supporting Information Figure S1. Heating of the bottom end of capillary (iii) using the coil on the capillary puller, causes the tip to partially liquefy and results in the axisymmetric narrowing of the opening based on power and time of heating. In this way, the initial 0.5 mm ID was narrowed in a flared manner to $\sim$ 0.2 mm. Each capillary was washed in acetone and dried to remove particulates. Capillaries (i) and (ii) were rinsed with toluene on the sections to be in contact with the organic dispersed phase and dried, while capillary (iii) was treated with O_2 plasma (Diener Electronic, Femto A) for 1 min to become temporarily hydrophilic, facilitating microdroplet production, and reduce wetting of the dispersed phase with capillary (iii). The treated capillaries were stored in DI water and used within 24 h after plasma treatment. After the fabrication and treatment of the capillaries, the flow-focusing device was assembled using PEEK T-junctions (0.05″ thru hole, IDEX Health and Sciences) and Teflon tubing (fluorinated ethylene propylene, FEP). Capillary (i) was connected to two T-junctions using 1/8″ ferrule fittings with Tygon tubing (1/8″ OD, 1/16″ ID, McMaster Carr) as an adapter between the glass capillary and the fitting. Capillary (i) was connected such that the bases of both T-junctions were perpendicular to the axis of the capillary. Capillaries (ii) and (iii) were adapted to 1/16″ ferrules using FEP tubing (1/16″ OD, 0.04″ ID, IDEX Health and Sciences), Capillary (ii) was fastened into the prepolymer mixture line while Capillary (iii) only required a small 1/16″ sleeve for fastening into the outlet side of the T-junction. Both inner capillaries were threaded through the axis of the T-junction to protrude coaxially into Capillary (i) with 1.5 mm of distance between the end of Capillary (ii) and the flame-tip of Capillary (iii). The dispersed phase lines flow into the side with Capillary (ii), while water and SDS flow into the base of the T-junction on the side of the reactor with Capillary (iii) acting as the outlet for the combined flow with formed elastomeric microparticles.

Reagent preparation

Continuous elastomeric microparticle synthesis within the constructed flow-focusing microreactor required three reagent lines: a cross-linking catalyst stream (Q_1) with composition ratio of Karstedt's catalyst to toluene (R_1), a polymer and cross-linker mixture (Q_2) with specific polymer to diene volumetric ratios (R_2), and an aqueous continuous phase (Q_3). See Table 1. Their respective inlet locations and flow-focusing characteristics are illustrated in Figure 2A.

The polymer and cross-linker stream (Q_2) was prepared by mixing the polymer (PHMS) and cross-linker (1,5-hexadiene) in predetermined ratios. For this work, we utilized R_2 ratios of 2, 5, 8, and 10. The cross-linking catalyst stream (Q_1) composition ratio R_1 was determined empirically for each R_2 by

Table 1. Stream Components of the Flow-Focusing Microreactor

Stream	Components	Purpose	Stream Variable	Operation Variable
Q_1	Toluene	Solvent and diluent	$R_1 = \frac{V_{\text{Karstedt}}}{V_{\text{Toluene}}}$	$R_{\text{PC}} = \frac{Q_2}{Q_1}$
	Karstedt's catalyst	Cross-linking catalyst		
Q_2	PHMS	Polymer	$R_2 = \frac{V_{\text{PHMS}}}{V_{\text{Hexadiene}}}$	
	1,5-Hexadiene	Cross-linker		
Q_3	Water	Continuous phase		
	Sodium dodecyl sulfate	Surfactant		

evaluating the polymerization time observed when 100 μL each of Q_1 and Q_2 were mixed in a 2-mL glass vial. Serial dilutions of a base catalyst solution (R_1 = 1:200 Karstedt's catalyst to toluene) were performed to run the gelation tests until a gelation time of ~5 min was achieved. Cross-linking time was recorded when the 200 μL of reacting mixture stopped flowing (i.e., the vial could be inverted with no movement of the bulk polymer). The continuous phase (Q_3) was prepared by adding 3 wt % SDS in DI water in a falcon tube, and placing the tube in an ultrasonic bath (Branson, CPX5800) for 2 min to expedite the dissolution process.

The three precursor solutions were loaded in glass, gas-tight syringes (SGE Analytical) and coupled to computer-controlled syringe pumps (Harvard Apparatus, PHD 2000 Ultra) for precise delivery to the flow-focusing microreactor. FEP tubing (IDEX Health and Sciences) served as the inlet line for the polymer stream (1/16″ OD, 0.04″ ID), as well as for the catalyst solution and continuous phase (1/16″ OD, 0.02″ ID). The microreactor was arranged vertically and supported by two clamps underneath an inverted microscope (Leica, M205C). A high-speed CMOS camera (FASTEC IL5) was used to characterize the microdroplet formation within the flow-focusing microreactor. Due to the vertical orientation of the constructed microreactor, an angled front-coated 50.8-mm optical mirror (Thorlabs) and external LED Illuminator (Nathaniel Group, Sugar CUBE Ultra) were implemented for bright-field optical microscopy. The setup was constructed on a self-leveling optical table (Thorlabs, PTS603) for vibration mitigation and stability.

Elastomeric microparticle production and collection

Figure 2B illustrates the microdroplet formation properties observed inside the flow-focusing microreactor described in "Elastomeric microparticle production microreactor construction" section. The cross-linking catalyst (Q_1) and the polymer and the cross-linker mixture (Q_2) streams constituted the dispersed phase. The aqueous surfactant solution (Q_3), infused at the opposite end of the system, directed the dispersed phase through the inner orifice and engulfed the polymerizing mixture through an oscillatory jetting regime (see Supporting Information Movie M-1). After Q_1 and Q_2 mix, the polymer begins cross-linking via hydrosilylation (see Supporting Information Figure S2). Emerging elastomeric microparticles were collected in 20-mL glass vials filled with DI water. The outlet stream was submerged beneath the water level to avoid deformation of partially cross-linked microdroplets while dropping from the outlet into the collection bath (Figure 2A [inset]). Elastomeric microparticles with a total volume of 200–1500 μL were synthesized for each R_1/R_2 pairing at the following volumetric polymer mixture to catalyst ratios (R_{PC}): 1:1, 1.5:1, 2:1, 2.5:1, and 3:1. In our preliminary tests, it was determined that the most consistent operation window for monodispersed production of PHMS microparticles within the flow-focusing microreactor was the dripping flow regime. The flow behavior at the droplet generating orifice is controlled by the relative flow rates of the combined dispersed phase ($Q_D = Q_1 + Q_2$) and the continuous phase (Q_3) to be further discussed later. In the dripping regime of a 3-D flow-focusing microreactor, the geometry of the constriction primarily controls the diameter of the microdroplet.[22–24] However, if the flow rate through the orifice is increased significantly, the flow of silicone elastomer switches to a jetting regime which results in polydispersity of the microdroplets due to the unstable nature of the viscous polymer jet at the transition state.

Following each trial, bright-field images of the resulting elastomeric microparticles at 5x, 10x, and 16x magnifications were acquired for characterization of the diameter and size distribution of the collected elastomeric microparticles. Then, multiple washes of water, IPA, acetone, and toluene were utilized, along with fine filter paper (Whatman, 2 μm pore size) to remove the surfactant and transfer the collected elastomeric microparticles from DI water to toluene. PHMS microparticle samples used only for imaging were treated with 12 mg/mL silver acetate (as an insoluble dye) prior to washing. Post-wash images at 5x, 10x, and 16x magnifications were then acquired to observe the swelling characteristics of the elastomeric microparticles. Although toluene will not be used in the exemplary cross-coupling reaction, it is an ideal solvent to characterize swelling behavior of PHMS as the high degree of swelling allows for more accurate characterization of slight differences in the PHMS network.

Videos of the microdroplet formation region were acquired for each tested ratio using the high-speed camera (Fastec IL5). A custom-developed MATLAB-based image processing code was utilized to automatically analyze the recorded images and provide temporal measurements for the microdroplet diameter, polydispersity, jet length, and production frequency inside the microreactor.

Elastomeric microparticle loading and characterization

Palladium was introduced into 1 g of elastomeric microparticles synthesized at R_2 = 5:1 and R_{PC} = 1:1 by dissolving 20 mg of Pd^{2+} acetate per gram of dry PHMS microparticles in toluene and giving enough time for the dissolved Pd ions to diffuse into the microparticles and be reduced to metallic Pd as detailed in Stibingerova et al. The Pd-loaded microparticles were then washed and packed into a 1/8″ OD 1/16″ ID FEP tube to be used as the μ-PBR. A 3-D focused ion beam-scanning electron microscope (FIB-SEM) in combination with transmission electron microscopy (TEM) were employed to confirm the presence of reduced Pd inside synthesized PHMS microparticles. The TEM samples were prepared by slicing and thinning a piece of the bulk microparticle until transparent to the electron beam. In addition, energy dispersive x-ray spectroscopy (EDS) was used for characterization of the loaded Pd in PHMS microparticles (see Supporting Information S3).

Microparticle-packed bed reactor

The washed Pd-loaded PHMS microparticles were transferred to a clean reaction solvent (80% ethanol in water) to be packed into a length of 1/8″ OD and 1/16″ ID FEP tubing. The microparticles were suspended in a vial of solvent by agitation as the solvent was withdrawn from the vial through the Teflon tubing and recovered in a gas-tight glass syringe loaded on a computer-controlled syringe pump. A 2-μm frit was placed at the end of the tube to allow solvent flow while retaining the microparticles in the μ-PBR. Once all the microparticles were transferred to the μ-PBR, solvent was flowed at 2 mL/min to maximize microparticle packing within the μ-PBR. The excess tubing was removed and the μ-PBR was weighed both with and without solvent to determine the void volume of the bed for residence time calculations.

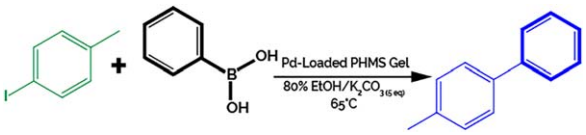

Reaction 1. Suzuki-Miyaura cross-coupling between 4-iodotoluene and phenylboronic acid, at 65°C in the presence of Pd-loaded PHMS gel with potassium carbonate as a base, forming 4-phenyltoluene.

[Color figure can be viewed at wileyonlinelibrary.com]

Continuous Suzuki-Miyaura cross-coupling reaction

The exemplary cross-coupling reaction was conducted using 4-iodotoluene in 80% ethanol and water, phenylboronic acid in 80% ethanol and water, and potassium carbonate (base) in 30% ethanol in water (Reaction 1 and Supporting Information S4 for full catalytic cycle). Naphthalene was used as an internal standard for the conversion and yield measurements. All three precursors were introduced to the μ-PBR at equal flow rates using a cross-junction (0.05″ thru hole, IDEX Health and Sciences) for residence times of 5, 10, and 30 min. Samples were collected at the reactor outlet and analyzed using high performance liquid chromatography (HPLC) with a gradient of water and acetonitrile for conversion and yield measurements. Individual chemical species were introduced to the HPLC column to determine elution time for each of the precursors, the naphthalene standard, and the 4-phenyltoluene product with the same water/acetonitrile gradient. Samples from the μ-PBR were collected every 10 min or every residence time (whichever was longer), until the reaction yield reached steady state.

Results and Discussion

Elastomeric microparticle synthesis and characterization

PHMS Jet Characteristics. One important parameter in the production of homogeneous and monodisperse microparticles is the *Damkohler* number which relates the rate of mixing within the microdroplets to the rate of the cross-linking reaction. A *Damkohler* number < 1 suggests that the microdroplets are completely mixed before the reaction proceeds appreciably. In this system, the mixing timescale in multiphase microfluidics [O(ms)][25,26] is far shorter than the reaction timescale as determined by the batch cross-linking tests [O(min)]. The behavior of the microdroplet forming jet was analyzed by applying a custom-developed microdroplet detection MATLAB script to the extracted frames acquired from the high-speed videos of the PHMS microdroplets forming in the flow-focusing microreactor. The image-processing code was then utilized to detect the diameter and production frequency of formed microdroplets, as well as the jet length. Example video detailing the various image processing steps is available in Supporting Information S5–S7 and Movie M-2. The observed trends of varying the ratio of the total dispersed phase flow rate ($Q_1 + Q_2 \equiv Q_D$) to the continuous phase flow rate ($Q_3 \equiv Q_C$) on the size and production frequency of microdroplets are consistent with previously reported flow-focusing geometries.[22,23,27–29] The diameter of the microdroplets increases with increasing Q_D/Q_C while the production

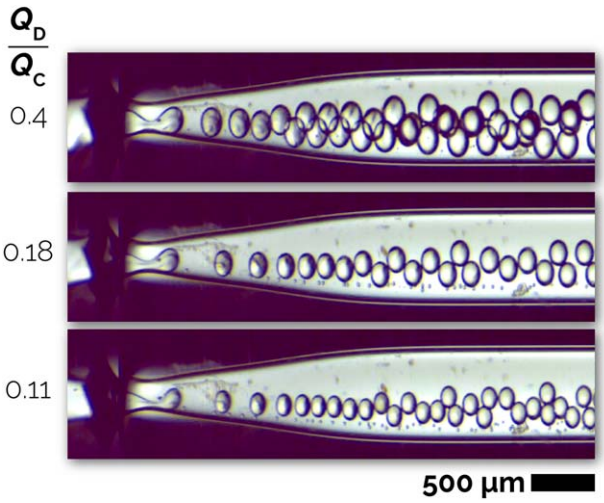

Figure 3. Sample micrographs extracted from high speed video showing the effect of dispersed to continuous flow rate ratio.

$R_2 = 8$, $R_{PC} = 1$, $Q_D = 16$ μL/min $Q_C = 40$, 90, and 150 μL/min. [Color figure can be viewed at wileyonlinelibrary.com]

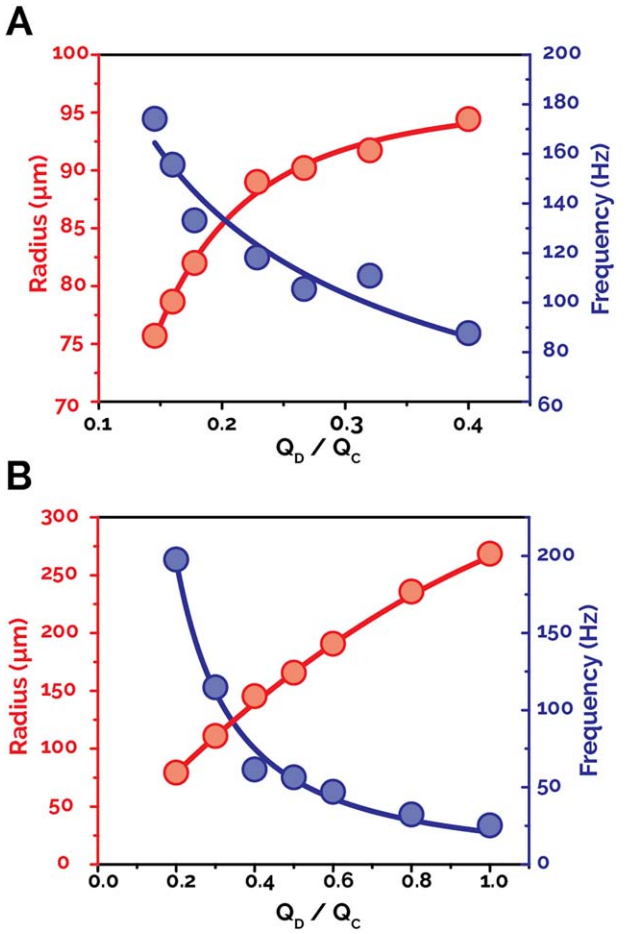

Figure 4. Characterization of the effect of the ratio of the dispersed phase to the continuous phase on the size and production frequency of PHMS microdroplets.

$R_2 = 8$ and $R_{PC} = 1$. (A) Constant dispersed phase flow rate, $Q_D = 16$ μL/min. (B) Constant continuous phase flow rate, $Q_C = 100$ μL/min. [Color figure can be viewed at wileyonlinelibrary.com]

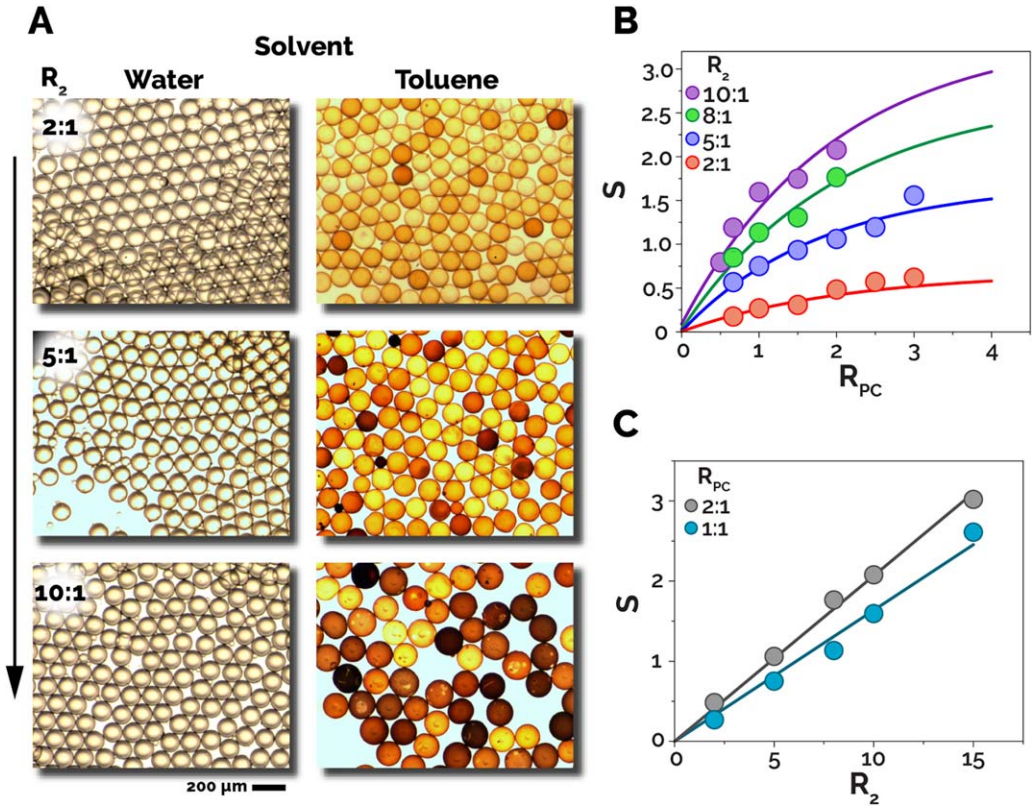

Figure 5. (A) Bright-field images of elastomeric microparticles in water and toluene. $R_2 = 2$, 5, and 10; $R_{PC} = 2{:}1$. (B) Swelling vs. polymer to catalyst mixture flow rate ratio (R_{PC}) for selected values of R_2. (C) Swelling vs. polymer to cross-linker ratio (R_2) for selected values of R_{PC}.

[Color figure can be viewed at wileyonlinelibrary.com]

frequency decreases. Snapshots of the microdroplet formation region at a constant dispersed phase flow rate and three different continuous phase flow rates are shown in Figure 3. The size of microdroplets at a constant Q_D decreases as Q_C increases, as can be seen in Figure 3. High-speed videos at each ratio of Q_D/Q_C are then analyzed using a custom droplet detection script in MATLAB to extract information about the jet and droplet formation. Figure 4A shows the effect of changing Q_C from 40 to 110 μL/min while maintaining Q_D constant at 16 μL/min ($R_{PC} = 2{:}1$). Figure 4B shows the effect of changing Q_D from 20 to 100 μL/min ($R_{PC} = 2{:}1$) while maintaining Q_C constant at 100 μL/min. Increasing Q_D increases the size of the droplets formed by the flow-focusing microreactor as more of the dispersed phase must flow through the opening to satisfy mass conservation. The larger size of microdroplets in Figure 4B compared to Figure 4A at the same value of Q_D/Q_C is due to the higher total volumetric phase of the dispersed phase, Q_D. The PHMS jet transitions through various flow regimes with increasing Q_C, from plug flow at low flow rates through droplet dripping up to jetting at high flow rates when the shear force on the fluid interface extends the jet past the neck of the constricted capillary (see Supporting Information Figure S8). In the next set of experiments, we studied the effect of the size of PHMS microparticles on their swelling index. It was observed that the swelling index was independent of the initial microparticle size, suggesting a uniform mesh network for different microparticles with a similar polymer to cross-linker ratio. The final microparticle diameter also depends on the initial cross-linking concentration as the particles contract as the cross-linking progresses with higher cross-linking concentrations contracting the most (see Supporting Information S9).

Swelling of Elastomeric Microparticles. Swelling of the produced silicone elastomer microparticles is an important characteristic, which may have implication on applications in both biomedical and organic synthesis fields. In biomedical applications, the swelling of elastomeric microparticles will affect the degree of drug uptake into the microparticles for initial loading and diffusion once administered to obtain optimal drug delivery kinetics.[30] In organic synthesis applications, the microparticles swelling will control both the loading of metal catalyst into the microparticle (i.e., microreaction scaffolds) and the rate and extent of metal-mediated chemical reaction. It would be desirable to completely immobilize the metal catalyst within the silicone elastomer microparticle with no leaching while allowing for fast diffusion of the solvent and reaction mixture to and from the active sites. The degree of swelling is largely controlled by the density of cross-linking bonds between PHMS backbones in the elastomer.[31] Theoretical models of the swelling of cross-linked networks exist,[32] however, they are generally long polymer chains with low cross-linking density. The cross-linked PHMS examined in this study has short chains (degree of polymerization ~40 monomers) and very dense cross-links (~1:5 mole ratio of cross links to backbone units). For this reason, the swelling was determined experimentally. Low density cross-linking results in a more elastic elastomer while high density cross-linking leads to a rigid elastomer. The parameters controlling the cross-linking density are the concentration of the cross-linker in the polymer mixture (R_2), and the ratio of the polymer to the cross-

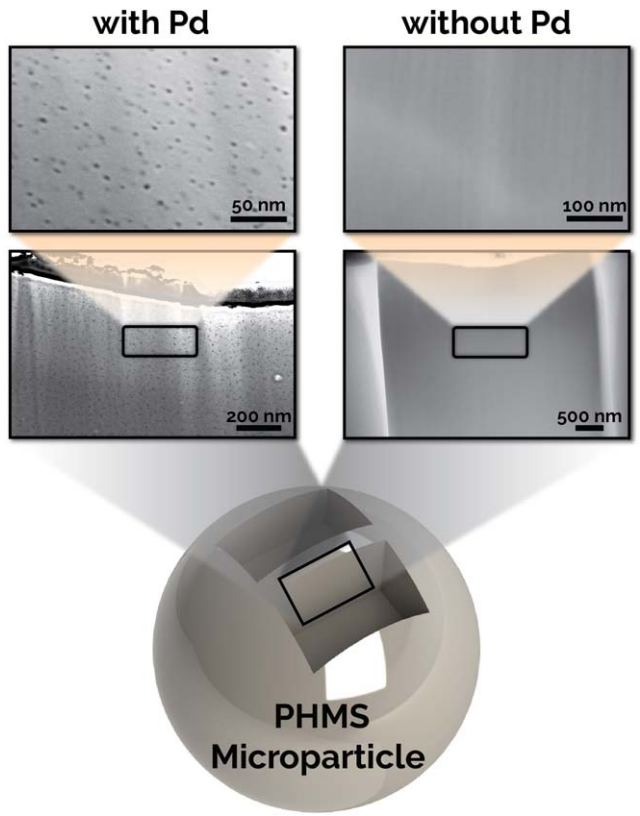

Figure 6. Bright-field TEM images of a FIB-produced slice of PHMS microparticle both with (left) and without (right) loading of Pd.

[Color figure can be viewed at wileyonlinelibrary.com]

linking catalyst mixture (R_{PC}). As R_{PC} decreases, the microparticles are already partially swollen with the catalyst dilution solvent (toluene) while the microdroplets finish the cross-linking reaction.

To study the effect of polymer to cross-linker ratio on the degree of swelling in the elastomeric microparticles, we measured the volume difference of collected PHMS microparticles before and after switching to an organic solvent. The size of the collected elastomeric microparticles was determined by applying a circle detection algorithm to images of a monolayer of microparticles at each combination of R_2 and R_{PC} in both aqueous (water) and organic (toluene) solvents (Figure 5A). We calculated the polydispersity and the swelling index of each sample of elastomeric microparticles from the histogram returned by the automatic circle detection algorithm (see Supporting Information Figure S10). Swelling index is defined as the change in microparticle volume upon switching from an aqueous to an organic solvent divided by the initial volume of the microparticles in the aqueous phase ($S = \frac{V_T - V_W}{V_W}$). As the PHMS microparticles are synthesized with toluene as the solvent for the catalyst stream to promote homogeneous mixing in the polymer jet, the swelling index studies were performed in toluene (good solvent for PHMS) as the swelling solvent. The swelling was also examined for the 80% ethanol and water mixture used as the reaction solvent for the cross-coupling reaction. However, both water and ethanol are poor solvents for PHMS and the network does not swell appreciably (less than 2% swelling; see Supporting Information S11). Therefore, as a measure of network elasticity, toluene was selected to perform the bulk of the swelling experiments. Although only toluene was used as an exemplary solvent for the microparticle swelling characterizations, the same procedure can be applied for other aqueous/organic solvents. The swelling index was analyzed as a function of R_2 and R_{PC}. The swelling ratio increases as both R_2 and R_{PC} increase, with the swelling ratio expected to plateau in the limit of pure elastomer mixture during the microdroplet formation (Figures 5B, C). As R_2 increases, the number of cross-linker bridges between PHMS polymer backbones is reduced, leading to a network that is more loosely connected. This allows for a greater uptake of solvent into the polymer network. At the relatively high cross-linker concentrations studied, the high number of cross-linked bonds per PHMS backbone results in a linear increase in swelling (Figure 5C), likely until the number of cross-linking bonds per polymer chain begins to approach O(1). As R_{PC} increases the concentration of polymer mixture vs. solvent increases within each droplet leading to an increase

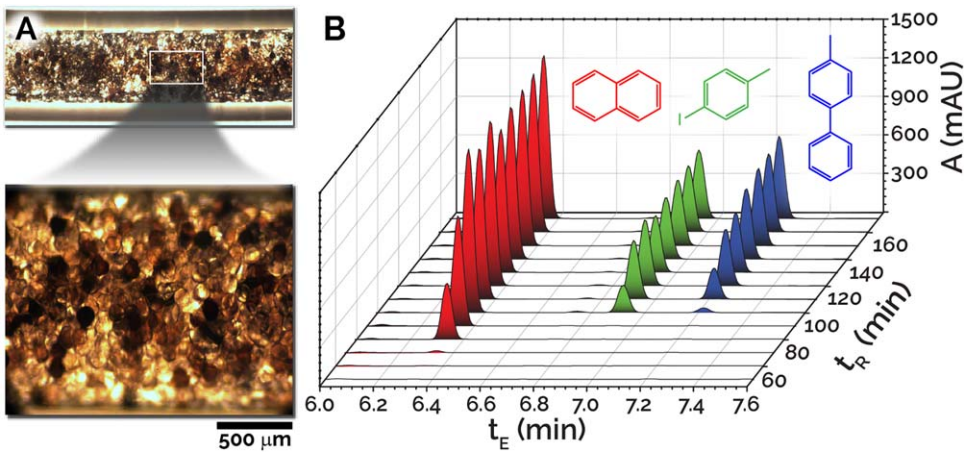

Figure 7. (A) Overview and enlarged view of μ-PBR made from 1/8″ OD, 1/16″ ID FEP Tubing. Scale bar is 200 μm. (B) Waterfall graph of HPLC traces taken every 10 min during startup.

Axes are column elution time (water and acetonitrile with 0.1% formic acid gradient), reaction time, and absorbance at 270 nm. Reaction conditions: temperature = 65°C, 4-iodotoluene (0.2 M), naphthalene (0.05 M), phenylboronic acid (0.3 M), and potassium carbonate (1 M). [Color figure can be viewed at wileyonlinelibrary.com]

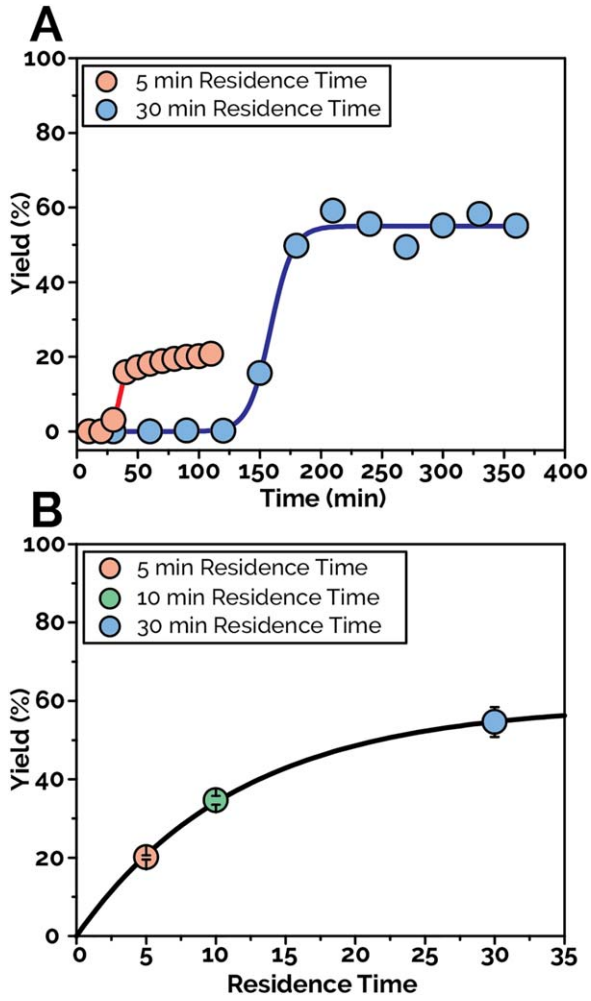

Figure 8. (A) Measured C-C cross-coupling yield during the start-up stage of μ-PBR for two residence times of 5 and 30 min and (B) at steady-state operation at the reaction temperature of 65°C.

The utilized μ-PBR had a total reactor volume (void) of 384 μL with a packing of 67%. [Color figure can be viewed at wileyonlinelibrary.com]

in maximum swelling. Microparticles with the same network composition have the same swelling ratio independent of absolute particle size.

Case study: μ-PBR for continuous Suzuki-Miyaura cross-coupling

To highlight an example of the applications of the PHMS microparticles in organic synthesis, we loaded the synthesized microparticles with Pd and used them as microreaction vessels in a μ-PBR for Suzuki-Miyaura cross-coupling reactions. By loading the Pd into the PHMS microparticles in toluene (when swollen) and then loading the particles into the μ-PBR in an aqueous 80% ethanol solution (with negligible swelling), we ensure that the reduced Pd remains within the microparticles. We confirmed the Pd loading in the PHMS microparticles by TEM microscopy (Figure 6) and energy dispersive x-ray spectroscopy (EDS). A TEM sample of a Pd-loaded elastomeric microparticle was prepared alongside a sample of unloaded PHMS microparticle showed the presence of Pd nanoparticles in the bulk of the microparticle (Figure 6). EDS was also performed on both the bulk Pd-loaded elastomeric microparticles and unloaded control microparticles, and Pd was detected only in the loaded microparticles at ~2 wt % (see Supporting Information Figure S3).

Figure 7A shows the constructed μ-PBR using Pd-loaded PHMS microparticles and a FEP tubing (1/8″ OD, 1/16″ ID). The inset of Figure 7A shows the packing of PHMS microparticles within the reactor after a 24-h continuous operation. Figure 7B shows initial startup saturation of the precursors and the internal standard (naphthalene) into the PHMS microparticles plus product formation up to steady state. During the startup of the μ-PBR, the microparticles in the bed begin to uptake the reactants and the product. Once the elastomeric microparticles are saturated with the chemical species, the species will elute from the μ-PBR. The species that are more hydrophobic have higher affinity for the silicone elastomer microparticles. As shown in Figure 7B, the chemical species are eluted from the μ-PBR in the order of their hydrophobicity. Once the column is fully saturated with reactants, the measured yield within the collected sample at the outlet of μ-PBR starts to increase until it reaches steady state (Figure 8A). The initial saturation time of the μ-PBR is influenced by the flow rates of the precursors fed to the reactor. As the volumetric flow rate of the precursors into the μ-PBR is increased, the convective mass-transport coefficient of the chemical species to and from the surface of the elastomeric microparticles is increased, resulting in an increased Biot number. The equilibrium concentration of chemical species within the PHMS microparticles of the μ-PBR remains constant at various volumetric flow rates, thus, the saturation limit of microparticles is reached at a shorter timescale at high precursor flow rates (e.g., 5 min residence time) compared to the low precursor flow rates (e.g., 30 min residence time). The reaction was conducted using residence times of 5, 10, and 30 min resulting in reaction yields of 20, 35, and 55% 4-phenyltoluene at steady state, respectively (Figure 8B).

To determine leaching of the catalyst from the microparticles into the reaction mixture inductively coupled plasma mass spectrometry (ICP-MS) analysis of solvent collected from the reactor effluent was analyzed. The concentration of Pd in the reactor effluent was determined to be less than 0.3 ppb. Additionally, control reactions in batch were performed with unloaded PHMS microparticles and reactor effluent solvent. Both control experiments showed no yield at residence times of 1 h at the same reaction conditions.

The combination of the nonlinear decrease in the reaction yield vs. time and a plateau of maximum yield below 100% in Figure 8B suggest that the higher observed reaction yield per unit residence time at relatively short residence times (i.e., higher flow rates) might be attributed to the higher rate of convective mass transport within the μ-PBR. Thus, enhancing the convective mass transport at the surface of the microparticles by increasing the flow rate and increasing the residence time by increasing the reactor length will both have positive effects on the maximum yield in the shortest residence time possible. After the initial reaction kinetic studies (Figure 8), the external mass transport with respect to the microparticles (i.e., through the voids) was decoupled from the residence time by splitting the μPBR into two equal segments. Intraparticle mass transport is primarily influenced by particle composition while external mass transport in the μ-PBR is primarily controlled by the reactor flow rates and operating conditions. In preliminary testing of these parameters, the packed bed was tested at

three different conditions: full length 10 min residence time (38.4 μL/min), half-length 5 min residence time (38.4 μL/min), and half-length 10 min residence time (19.2 μL/min). When the reaction was conducted at the same flow rate (halved residence time) in the half-length μPBR the yield was decreased by $\sim$50%. When the residence time was remained constant (halved flow rate) the reaction yield was lower than the full-length reactor (i.e., higher flow rate). Thus, the biphasic cross-coupling reaction yield could be further improved by increasing the length (i.e., increasing total bed volume) of the μ-PBR, resulting in a higher flow rate to achieve a given residence time and increased mass-transport rates. Further experimental studies are underway and will be coupled with mass-transport modeling efforts to optimize more thoroughly the PHMS microparticles properties and reactor operating conditions in order to maximize conversion for a range of cross-coupling substrates.

As a preliminary case study, the development of a continuous flow C-C cross-coupling strategy with a promising yield of 60% at a 30 min residence time warrants additional process development and reaction optimization. In addition, it should be noted that continuous flow chemistry strategies enable enhanced process control and stability as compared to batch methods. Moreover, the Pd-loaded microparticles remove the need for expensive and energy-intensive catalyst recovery step from the reaction media. The long-term stability of the PHMS-based Pd catalysts is also a significant benefit over its homogeneous counterparts; the same μ-PBR has been used for several days of continuous run over the course of several months without replacing the microparticles. The PHMS microparticle catalyst used in the reaction has the benefit of performing the reaction using environmentally friendly solvents featuring ethanol and water mixtures instead of more toxic and volatile solvents that are currently being used in the chemical industry (e.g., tetrahydrofuran, toluene, hexane, dioxane, or dichloromethane).

Conclusion

In this work, we demonstrated a novel method for the on-chip synthesis of chemical cross-linkable silicone elastomer microparticles with tunable size, production frequency, and swelling characteristics. The developed microfluidic platform enabled simultaneous formation and chemical cross-linking of silicone elastomer microdroplets on-chip, using an off-the-shelf assembled flow-focusing microreactor. The developed continuous flow chemistry strategy could be utilized for developing a library of other chemically cross-linked polymer and cross-linker pairs for applications in organic synthesis, targeted drug delivery, cell encapsulation, or biomedical imaging.

An application of the silicone elastomer microparticles is demonstrated by performing organic synthesis of 4-phenyltoluene using the PHMS microparticles as catalyst scaffolds for loading the Pd nanoparticles. The loading of Pd in PHMS microparticles instead of bulk PHMS allowed for the continuous operation of Suzuki-Miyaura chemistry using a μ-PBR. Further work in this area could involve tuning the elastomeric microparticle properties (e.g., swelling, size, Pd-loading, and the structure of the cross-linker), the μ-PBR properties (e.g., packing fraction, mass-transfer characteristics, and reactor volume), and the reaction conditions (e.g., temperature, concentration, and chemical species) to optimize the reaction yield for a desired cross-coupling reaction.

Acknowledgments

The authors would like to acknowledge the support from NC State University. The authors also acknowledge the North Carolina State University Analytical Instrument Facility for the use of their Quanta 3-D FIB-SEM, Verios SEM, and TEM instruments. The authors declare no competing financial interest.

Literature Cited

1. Ruiz-Castillo P, Buchwald SL. Applications of palladium-catalyzed C-N cross-coupling reactions. *Chem Rev*. 2016;116(19):12564–12649.
2. Adamo A, Beingessner RL, Behnam M, Chen J, Jamison TF, Jensen KF, Monbaliu J-CM, Myerson AS, Revalor EM, Snead DR, Stelzer T, Weeranoppanant N, Wong SY, Zhang P. On-demand continuous-flow production of pharmaceuticals in a compact, reconfigurable system. *Science*. 2016;352(6281):61–67.
3. Jensen KF. Flow chemistry-microreaction technology comes of age. *AIChE J*. 2017;63(3):858–869.
4. Stibingerova I, Voltrova S, Kocova S, Lindale M, Srogl J. Modular approach to heterogenous catalysis. Manipulation of cross-coupling catalyst activity. *Org Lett*. 2016;18(2):312–315.
5. Winterberg M, Tsotsas E. Impact of tube-to-particle-diameter ratio on pressure drop in packed beds. *AIChE J*. 2000;46(5):1084–1088.
6. Martino C, Lee TY, Kim S-H, DeMello AJ. Microfluidic generation of PEG-b-PLA polymersomes containing alginate-based core hydrogel. *Biomicrofluidics*. 2015;9(2):024101.
7. Shepherd RF, Conrad JC, Rhodes SK, Link DR, Marquez M, Weitz DA, Lewis JA. Microfluidic assembly of homogeneous and Janus colloid-filled hydrogel granules. *Langmuir*. 2006;22(21):8618–8622.
8. Peppas NA, Bures P, Leobandung W, Ichikawa H. Hydrogels in pharmaceutical formulations. *Eur J Pharm Biopharm*. 2000;50(1):27–46.
9. Slaughter BV, Khurshid SS, Fisher OZ, Khademhosseini A, Peppas NA. Hydrogels in regenerative medicine. *Adv Mater*. 2009;21(32–33):3307–3329.
10. Khademhosseini A, Langer R. Microengineered hydrogels for tissue engineering. *Biomaterials*. 2007;28(34):5087–5092.
11. Peppas NA, Hilt JZ, Khademhosseini A, Langer R. Hydrogels in biology and medicine: from molecular principles to bionanotechnology. *Adv Mater*. 2006;18(11):1345–1360.
12. Tumarkin E, Kumacheva E. Microfluidic generation of microgels from synthetic and natural polymers. *Chem Soc Rev*. 2009;38(8):2161–2496.
13. Cho S, Li Y, Seo M, Kumacheva E. Nanofibrillar stimulus-responsive cholesteric microgels with catalytic properties. *Angew Chem Int Ed Engl*. 2016;55(45):14014–14018.
14. Chau M, Abolhasani M, Thérien-Aubin H, Li Y, Wang Y, Velasco D, Tumarkin E, Ramachandran A, Kumacheva E. Microfluidic generation of composite biopolymer microgels with tunable compositions and mechanical properties. *Biomacromolecules*. 2014;15(7):2419–2425.
15. Wang Y, Tumarkin E, Velasco D, Abolhasani M, Lau W, Kumacheva E. Exploring a direct injection method for microfluidic generation of polymer microgels. *Lab on a Chip*. 2013;13(13):2547–2553.
16. Shah RK, Kim J, Agresti JJ, Weitz DA, Chu L. Fabrication of monodisperse thermosensitive microgels and gel capsules in microfluidic devices. *Soft Matter*. 2008;4(12):2303–2309.
17. Baah D, Floyd-Smith T. Microfluidics for particle synthesis from photocrosslinkable materials. *Microfluid Nanofluid*. 2014;17(3):431–455.
18. Rossow T, Heyman JA, Ehrlicher AJ, Langhoff A, Weitz DA, Haag R, Seiffert S. Controlled synthesis of cell-laden microgels by radical-free gelation in droplet microfluidics. *J Am Chem Soc*. 2012;134(10):4983–4989.
19. Zhang J, Teixeira AR, Kögl LT, Yang L, Jensen KF. Hydrodynamics of gas–liquid flow in micropacked beds: pressure drop, liquid holdup, and two-phase model. *AIChE J*. 2017;63(10):4694–4611.
20. Zhang J, Teixeira AR, Jensen KF. Automated measurements of gas-liquid mass transfer in micro-packed bed reactors. *AIChE J*. 2018;64(2):564–570.
21. Hu C, Hartman RL. High-throughput packed-bed microreactors with in-line analytics for the discovery of asphaltene deposition mechanisms. *AIChE J*. 2014;60(10):3534–3546.
22. Nie Z, Seo M, Xu S, Lewis PC, Mok M, Kumacheva E, Whitesides GM, Garstecki P, Stone HA. Emulsification in a microfluidic flow-

focusing device: effect of the viscosities of the liquids. *Microfluid Nanofluid.* 2008;5(5):585–594.
23. Anna SL, Bontoux N, Stone HA. Formation of dispersions using "flow focusing" in microchannels. *Appl Phys Lett*. 2003;82(3):364–366.
24. Stone HA, Stroock AD, Ajdari A. Engineering flows in small devices. *Annu Rev Fluid Mech*. 2004;36(1):381–411.
25. Song H, Bringer MR, Tice JD, Gerdts CJ, Ismagilov RF. Experimental test of scaling of mixing by chaotic advection in droplets moving through microfluidic channels. *Appl Phys Lett*. 2003;83(22):4664–4666.
26. Tice JD, Song H, Lyon AD, Ismagilov RF. Formation of droplets and mixing in multiphase microfluidics at low values of the Reynolds and the Capillary numbers. *Langmuir*. 2003;19(22):9127–9133.
27. Takeuchi BS, Garstecki P, Weibel DB, Whitesides GM. An axisymmetric flow-focusing microfluidic device. *Adv Mater*. 2005;17(8):1067–1072.
28. Xu S, Nie Z, Seo M, Lewis P, Kumacheva E, Stone HA, Garstecki P, Weibel DB, Gitlin I, Whitesides GM. Generation of monodisperse particles by using microfluidics: control over size, shape, and composition. *Angew Chem Int Ed Engl*. 2005;117(5):734–738.
29. Seo M, Paquet C, Nie Z, Xu S, Kumacheva E. Microfluidic consecutive flow-focusing droplet generators. *Soft Matter*. 2007;3(8):986–992.
30. Langer R, Peppas NA. Advances in biomaterials, drug delivery, and bionanotechnology. *AIChE J*. 2003;49(12):2990–3006.
31. Lee JN, Park C, Whitesides GM. Solvent compatibility of poly(dimethylsiloxane)-based microfluidic devices. *Anal Chem.* 2003;75(23):6544–6554.
32. Peppas NA, Merrill EW. Crosslinked poly(vinyl alcohol) hydrogels as swollen elastic networks. *J Appl Polym Sci*. 1977;21(7):1763–1770.

Manuscript received Dec. 8, 2017, and revision received Feb. 3, 2018.